



1 **Recent increases in the atmospheric growth rate and emissions of HFC-23**
2 **(CHF₃) and the link to HCFC-22 (CHClF₂) production.**

3 Peter G. Simmonds¹, Matthew. Rigby¹, Archie. McCulloch¹, Martin. K. Vollmer², Stephan.
4 Henne², Jens. Mühle³, Simon. O'Doherty¹, Alistair. J. Manning⁴, Paul. B. Krummel⁵, Paul. J.
5 Fraser⁵, Dickon. Young¹, Ray. F. Weiss³, Peter. K. Salameh³, Chris. M. Harth³, Stephan.
6 Reimann², Cathy. M. Trudinger⁵, Paul. Steele⁵, Ray. H. J. Wang⁶, Diane. J. Ivy⁷, Ron. G. Prinn⁷,
7 Blagoj. Mitrevski⁵, and David. M. Etheridge⁵.

8
9 ¹ Atmospheric Chemistry Research Group, University of Bristol, Bristol, UK

10 ² Empa, Swiss Federal Laboratories for Materials Science and Technology, Laboratory for Air
11 Pollution and Environmental Technology, Dübendorf, Switzerland,

12 ³ Scripps Institution of Oceanography (SIO), University of California, San Diego, La Jolla,
13 California, USA

14 ⁴ Met Office Hadley Centre, Exeter, UK

15 ⁵ Climate Science Centre, CSIRO Oceans and Atmosphere, Aspendale, Victoria, Australia

16 ⁶ School of Earth, and Atmospheric Sciences, Georgia Institute of Technology, Atlanta, Georgia,
17 USA

18 ⁷ Center for Global Change Science, Massachusetts Institute of Technology, Cambridge,
19 Massachusetts, USA.

20

21 Correspondence to: P.G. Simmonds (petersimmonds@aol.com)

22

23 **Abstract**

24 High frequency measurements of the potent hydrofluorocarbon greenhouse gas CHF₃
25 (HFC-23), a by-product of production of the hydrochlorofluorocarbon HCFC-22 (CHClF₂), at
26 five core stations of the Advanced Global Atmospheric Gases Experiment (AGAGE) network,
27 combined with measurements of firn and Cape Grim Air Archive (CGAA) air samples, are used
28 to explore the changing atmospheric abundance of HFC-23. These measurements are used in
29 combination with the AGAGE 2-D atmospheric 12-box model and a Bayesian inversion
30 methodology to determine model atmospheric mole fractions and the atmospheric history of
31 global HFC-23 emissions. The global modelled annual mole fraction of HFC-23 in the
32 background atmosphere was 28.9 ± 0.6 pmol mol⁻¹ at the end of 2016, representing a 28%
33 increase from 22.6 ± 0.4 pmol mol⁻¹ in 2009. Over the same time frame, the modelled mole
34 fraction of HCFC-22 increased by 19% from 199 ± 2 pmol mol⁻¹ to 237 ± 2 pmol mol⁻¹.
35 However, the annual average HCFC-22 growth rate decelerated from 2009 to 2016 at an annual
36 average rate of 0.5 pmol mol⁻¹ yr⁻².

37 Our results demonstrate that, following a minimum in HFC-23 global emissions in 2009
38 of 9.6 ± 0.6 Gg yr⁻¹, emissions increased to a maximum in 2014 of 14.5 ± 0.6 Gg yr⁻¹, declining
39 to 12.7 ± 0.6 Gg yr⁻¹ (157 Mt CO₂-eq. yr⁻¹) in 2016. The 2009 emissions minimum is consistent
40 with estimates based on national reports and is likely a response to the implementation of the
41 Clean Development Mechanism (CDM) to mitigate HFC-23 emissions by incineration in



42 developing (Non-Annex 1) countries under the Kyoto Protocol. Our derived cumulative
43 emissions of HFC-23 during 2010-2016 were 89 ± 2 Gg (1.1 ± 0.2 Gt CO₂-eq), which led to an
44 increase in radiative forcing of 1.0 ± 0.1 mW m⁻². Although the CDM had reduced global HFC-
45 23 emissions, it cannot now offset the radiative forcing of higher emissions from increasing
46 HCFC-22 production in Non-Annex 1 countries, as the CDM was closed to new entrants in
47 2009. We also find that the cumulative European HFC-23 emissions from 2010 to 2016 were
48 ~1.3 Gg, corresponding to just 1.5% of cumulative global HFC-23 emissions over this same
49 period.

50 1. Introduction

51 Due to concerns about climate change trifluoromethane (CHF₃, HFC-23) has attracted
52 interest as a potent greenhouse gas with a 100-yr global warming potential (GWP) of 12400
53 (Myhre et al., 2013) and an atmospheric lifetime of ~228 yr (SPARC, 2013). Unlike most
54 hydrofluorocarbons (HFCs) that have been introduced as replacements for ozone-depleting
55 chlorofluorocarbons (CFCs) and hydrochlorofluorocarbons (HCFCs), for example, HFC-134a as
56 a direct replacement for CFC-12, HFC-23 is primarily an unavoidable by-product of
57 chlorodifluoromethane HCFC-22 (CHClF₂) production due to the over-fluorination of
58 chloroform (CHCl₃). Most HFC-23 has historically simply been vented to the atmosphere
59 (UNEP, 2017a). HFC-23 has also been used as a feed-stock in the production of Halon-1301
60 (CBrF₃) (Miller and Batchelor, 2012) which substantially decreased with the phase-out of halons
61 in 2010 under the Montreal Protocol (MP), a landmark international agreement designed to
62 protect the stratospheric ozone layer. HFC-23 also has minor emissive uses in air conditioning,
63 fire extinguishers, and semi-conductor manufacture (McCulloch and Lindley, 2007) and very
64 minor emissions from aluminium production (Fraser et al., 2013). For developed countries HFC-
65 23 emissions were controlled as part of the “F-basket” under the Kyoto Protocol, an international
66 treaty among industrialized nations that sets mandatory limits on greenhouse gas emissions,
67 (https://ec.europa.eu/clima/policies/f-gas_en).

68 HCFC-22 is principally used in air-conditioning and refrigeration, as a component in
69 foam blowing and as a chemical feedstock in the manufacture of fluoropolymers, such as
70 polytetrafluoroethylene (PTFE). HCFC-22 production and consumption (excluding feedstock use)
71 are also controlled under the MP.

72 In the context of this paper we discuss “developed” and “developing” countries which we
73 take to be synonymous with Annex 1 (Non-Article 5) countries and Non-Annex 1 (Article 5)
74 countries, respectively.



75 Oram et al. (2008) measured HFC-23 by gas chromatography-mass spectrometry (GC-
76 MS) analysis of sub-samples the Cape Grim Air Archive (CGAA) spanning the period from
77 1978-1995 and reported a dry-air atmospheric abundance of 11 pmol mol^{-1} in late 1995. A top-
78 down HFC-23 emissions history and a comprehensive bottom-up estimate of global HFC-23
79 emissions were reported by Miller et al. (2010) using AGAGE observations (2007-2009) and
80 samples from the CGAA (1978-2009). Montzka et al. (2010), using measurements of firn air
81 from the permeable upper layer of an ice sheet and ambient air collected during three
82 expeditions to Antarctica between 2001 and 2009, constructed a consistent Southern Hemisphere
83 (SH) atmospheric history of HFC-23. Remote sensing observations of HFC-23 in the upper
84 troposphere and lower stratosphere by two solar occultation instruments have also been reported
85 (Harrison et al., 2011), indicating an abundance growth rate of $5.8 \pm 0.3\%$ per year, similar to
86 the CGAA surface trend of $5.7 \pm 0.4\%$ per year over the same period, (1989-2007). They also
87 determined that the absolute HFC-23 volume mixing ratio was 30% larger than ground based
88 measurements, most likely due to spectroscopic errors in the forward model. The spectra are
89 referenced to pressure mixtures of HFC-23 in pure nitrogen (N_2), so are likely reported in an
90 approximate volume mixing ratio scale, however, pressure-broadening effects could lead to a
91 significant calibration bias (Harrison et al., 2012).

92 Technical solutions to mitigate HFC-23 emissions, associated with HCFC-22 production,
93 have included optimisation of the process and voluntary and regulatory incineration in developed
94 (Annex 1) countries. Mitigation in developing countries (Non-Annex 1) has been introduced
95 under the United Nations Framework Convention on Climate Change's (UNFCCC's) Clean
96 Development Mechanism (CDM) to destroy HFC-23 from HCFC-22 production facilities
97 (UNEP, 2017a). This allowed certain HCFC-22 production plants in developing countries to be
98 eligible to provide Certified Emission Reduction (CER) credits for the destruction of the co-
99 produced HFC-23. Beginning in 2003 there were 19 registered HFC-23 incineration projects in
100 five developing countries with the number of projects in each country shown in parenthesis,
101 China (11), India (5), Korea (1), Mexico (1) and Argentina (1) (Miller et al., 2010). The first
102 CER credits under the CDM for HFC-23 abatement in HCFC-22 plants were approved in 2003
103 with funding through 2009. However, the CDM projects cover only about half of the HCFC-22
104 production in developing countries. The substantial reduction in global HFC-23 emissions
105 during 2007-2009 was attributed by Miller et al. (2010) to the destruction of HFC-23 by CDM
106 projects. In a subsequent paper, Miller and Kuijpers (2011) predicted future increases in HFC-23
107 emissions by considering three scenarios: a reference case with no additional abatement, and two
108 opposing abatement measures, less mitigation and best practice involving increasing application
109 of mitigation through HFC-23 incineration. Historically there has been a lack of information



110 about HFC-23 emissions from the non-CDM HCFC-22 production plants, although Fang et al.
111 (2014, 2015) recently provided a top-down estimate of HFC-23/HCFC-22 co-production ratios
112 in non-CDM production plants. They reported that the HFC-23/HCFC-22 co-production ratios in
113 all HCFC-22 production plants were $2.7\% \pm 0.4$ by mass in 2007, consistent with values
114 reported to the Executive Committee of the MP (UNEP, 2017a)

115 Here we use the high frequency atmospheric observations of HFC-23 and HCFC-22
116 abundances measured by GC-MS at the five longest-running remote sites of the Advanced
117 Global Atmospheric Gases Experiment (AGAGE). The site coordinates and measurement time
118 frames of HFC-23 and HCFC-22 are listed in Table 1. To extend our understanding of the long-
119 term growth rate of HFC-23, we combine the direct AGAGE atmospheric observations with
120 results from an analysis of firn air collected in Antarctica and Greenland and archived air from
121 the CGAA. The AGAGE 2-D 12-box model and a Bayesian inversion technique are used to
122 produce global emission estimates for HFC-23 and HCFC-22 (Cunnold et al., 1983; Rigby et al.,
123 2011, 2014). We also include observations from the AGAGE Jungfraujoch station to determine
124 estimates of European HFC-23 emissions (see section 3.2)

125

126 2. Methodology

127 2.1. AGAGE Instrumentation and Measurement Techniques

128 Ambient air measurements of HFC-23 and HCFC-22 at each site are recorded using the
129 AGAGE GC-MS-Medusa instrument which employs an adsorbent-filled ((HayeSep D)
130 microtrap cooled to $\sim -175^{\circ}\text{C}$ to pre-concentrate the analytes during sample collection (Miller et
131 al., 2008; Arnold et al., 2012). Samples are analysed approximately every 2 hours and are
132 bracketed by measurements of quaternary standards (see below) to correct for short-term drifts
133 in instrument response.

134 Typically for each measurement, the analytes from two litres of air are collected on the
135 microtrap and, after fractionated distillation, purification and transfer, are desorbed onto a single
136 main capillary chromatography column (CP-PoraBOND Q, 0.32 mm ID \times 25 m, 5 μm , Agilent
137 Varian Chrompack, batch-made for AGAGE applications) purged with helium (grade 6.0) that is
138 further purified using a heated helium purifier (HP2, VICI, USA). Separation and detection of
139 the compounds are achieved by using Agilent Technology GCs (model 6890N) and quadrupole
140 mass spectrometers in selected ion mode (initially model 5973 series, progressively converted to
141 5975C over the later years).

142 The quaternary standards are whole-air samples, pressurized into 34 L internally
143 electropolished stainless steel canisters (Essex Industries, USA). They are filled by the



144 responsible station scientist and/or on-site station personnel who are in charge of the respective
145 AGAGE remote sites using modified oil-free diving compressors (SA-3 and SA-6, RIX
146 Industries, USA) to ~60 bar (older canisters to ~40 bar). Cape Grim is an exception, where the
147 canisters used for quaternary standard purposes are filled cryogenically. This method of
148 cryogenically collecting large volumes of ambient air is the same as that is used for collecting air
149 for the CGAA and measurements of many atmospheric trace species in air samples collected in
150 this manner show that the trace gas composition of the air is well preserved (Fraser et al., 1991,
151 2016; Langenfelds et al., 1996, 2003). The on-site quaternary standards are compared weekly to
152 tertiary standards from the central calibration facility at the Scripps Institution of Oceanography
153 (SIO) in order to propagate the primary calibration scales and assess any long-term drifts. These
154 tertiary standards are filled with ambient air in Essex canisters under “baseline” clean air
155 conditions at Trinidad Head or at La Jolla (California) and are measured at SIO against
156 secondary ambient air standards (to obtain an “out” value) before they are shipped to individual
157 AGAGE sites. We define “baseline” as air masses that are representative of the unpolluted
158 marine boundary layer, uninfluenced by recent local or regional emissions. After their on-site
159 deployment they are again measured at SIO to obtain an “in” value, to assess any possible drifts.
160 They are also measured on-site against the previous and next tertiaries. The secondary standards
161 and the synthetic primary standards at SIO provide the core of the AGAGE calibration system
162 (Prinn et al, 2000; Miller et al., 2008).

163 The GC-MS-Medusa measurement precisions for HFC-23 and HCFC-22 are determined
164 as the precisions of replicate measurements of the quaternary standards over twice the time
165 interval as for sample-standard comparisons (Miller et al., 2008). Accordingly, they are upper-
166 limit estimates of the precisions of the sample-standard comparisons. Typical daily precisions
167 for each compound vary with abundance and individual instrument performance over time.
168 Average percentage relative standard deviation (% RSD) between 2007 and 2016 were: HFC-23
169 (0.1%-1.9%, average 0.7%); and for HCFC-22 (0.1%-2.5%, average 0.6%).

170

171 2.2. Firm and Archived Air

172 We used archived air samples from firm and in canisters to reconstruct an atmospheric
173 HFC-23 history. Firm air samples from Antarctica and Greenland were analyzed for HFC-23
174 using the same technology as the *in situ* measurements, details are provided in Supplementary
175 Material (2). The Antarctic samples were collected at the DSSW20K site in 1997-1998
176 (Trudinger et al., 2002) and include one deep sample at South Pole collected in 2001 (Butler et
177 al., 2001). Greenland samples were collected at the NEEM (North Greenland Eemian Ice
178 Drilling) site in 2008 (Buizert et al., 2012). The most recent version of the CSIRO firm model



179 was used to derive age spectra for the individual samples and more details on these samples and
180 their analysis are given in Vollmer et al. (2016, 2017) and Trudinger et al. (2016).

181 A diffusion coefficient of HFC-23 relative to CO₂ of 0.797 was used (Fuller et al., 1966).

182 CGAA measurements from three separate analysis periods were also used for the
183 reconstruction of past HFC-23 abundances. The CGAA samples have been collected since 1978
184 at the Cape Grim Air Pollution Station and amount to >130 samples in mostly internally
185 electropolished stainless steel canisters. Samples were analysed under varying conditions in
186 2006, 2011, and 2016. Here we use a composite of the results from these measurement sets.
187 Details of this are given in the Supplementary Material (2) and by Vollmer et al., (2017).

188 2.3. Calibration Scales

189 The estimated accuracies of the calibration scales for HFC-23 and HCFC-22 are
190 discussed below and a more detailed discussion of the measurement techniques and calibration
191 procedures are reported elsewhere (Miller et al., 2008; O'Doherty et al., 2009; Mühle et al.,
192 2010). HFC-23 and HCFC-22 measurements from all AGAGE sites are reported relative to
193 the SIO-07 and SIO-05 primary calibration scales, respectively, which are defined by suites of
194 standard gases prepared by diluting gravimetrically prepared analyte mixtures in N₂O to near-
195 ambient levels in synthetic air (Prinn et al., 2000; Miller et al., 2008).

196 The absolute accuracies of these primary standard scales are uncertain because possible
197 systematic effects are difficult to quantify or even identify. Combining known statistical and
198 systematic uncertainties, such as measurement and propagation errors, and quoted reagent
199 purities, generally yields lower uncertainties than are supported by comparisons among
200 independent calibration scales (Hall et al., 2014). Furthermore, some systematic uncertainties
201 may be normally distributed, while others like reagent purity are skewed in one direction.
202 Estimates of absolute accuracy are nevertheless needed for interpretive modelling applications,
203 and in this work, they are liberally estimated at -3%, +2% for HFC-23 and ±1% for HCFC-22.

204 2.4. Selection of baseline data

205 Baseline *in situ* monthly mean HFC-23 and HCFC-22 mole fractions were calculated by
206 excluding values enhanced by local and regional pollution influences, as identified by the
207 iterative AGAGE pollution identification algorithm (for details see Appendix in O'Doherty et
208 al., 2001). Briefly, baseline measurements are assumed to have Gaussian distributions around the
209 local baseline value, and an iterative process is used to filter out the points that do not conform
210 to this distribution. A second-order polynomial is fitted to the subset of daily minima in any 121-
211 day period to provide a first estimate of the baseline and seasonal cycle. After subtracting this



212 polynomial from all the observations a standard deviation and median are calculated for the
213 residual values over the 121-day period. Values exceeding three standard deviations above the
214 baseline are thus identified as non-baseline (polluted) and removed from further consideration.
215 The process is repeated iteratively to identify and remove additional non-baseline values until
216 the new and previous calculated median values agree within 0.1%.

217 2.5. Bottom-up emissions estimates

218 The sources of information on production and emissions of HFCs are generally incomplete
219 and do not provide a comprehensive database of global emissions. In Supplementary Material 1,
220 we compile global HCFC-22 production and HFC-23 emissions data. HCFC-22 is used in two
221 ways: (1) dispersive applications, such as refrigeration and air conditioning, whose production is
222 controlled under the Montreal Protocol and reported by countries as part of their total HCFC
223 production statistics, and (2) feedstock applications in which HCFC-22 is a reactant in chemical
224 processes to produce other products. Although there is an obligation on countries to report
225 HCFC-22 feedstock use to UNEP, this information is not made public. HCFC-22 production for
226 dispersive uses was calculated from the UNEP HCFC database (UNEP, 2017b) and the Montreal
227 Protocol Technology and Economic Assessment Panel 2006 Assessment (TEAP, 2006).
228 Production for feedstock use was estimated using trade literature as described in the
229 Supplementary Material S1 and the sum of production for dispersive and feedstock uses is
230 shown in Table S1.

231 HFC-23 emissions from Annex 1 countries are reported as a requirement of the
232 UNFCCC. Table S2 shows the total annual HFC-23 emissions reported by these countries
233 (UNFCCC, 2017). These include emissions from use of HFC-23 in applications such as semi-
234 conductor manufacture and fire suppression systems. These minor uses of HFC-23, originally
235 produced in a HCFC-22 plant, will result in the eventual emission of most or all into the
236 atmosphere and emissions have remained relatively constant at 0.13 ± 0.01 Gg yr⁻¹, a maximum
237 of 10% of all emissions (UNFCCC, 2017). Non-Annex 1 countries listed in Table S2 were
238 eligible for financial support for HFC-23 destruction under the CDM. Their emissions were
239 calculated by applying factors to their estimated production of HCFC-22 and offsetting this by
240 the amount destroyed under CDM, as described in the Supplementary Material (1). We discuss
241 these independent emission estimates because they are useful as *a priori* data constraints
242 (“bottom-up” emission estimates) which we compare to observation-based “top-down”
243 estimates.

244

245



246 2.6. Global atmospheric model

247 Emissions were estimated using a Bayesian approach in which our *a priori* estimates of
248 the emissions growth rate were adjusted by comparing modelled baseline mole fractions to the
249 atmospheric observations (Rigby et al., 2011; 2014). The firm air measurements were included in
250 the inversion, with the age spectra from the firm model used to relate the firm measurements to
251 high-latitude atmospheric mole fraction (Trudinger et al., 2016; Vollmer et al., 2016). A 12-box
252 model of atmospheric transport and chemistry was used to simulate baseline mole fractions,
253 which assumed that the atmosphere was divided into four zonal bands (30-90°N, 0-30°N, 30-0°S,
254 90-30°S) and at 500hPa and 200hPa vertically (Cunnold et al., 1994; Rigby et al., 2013). The
255 temperature-dependent rate constant for reaction with the hydroxyl radical (OH) was taken from
256 Burkholder et al. (2015), which led to a lifetime of 237 yr using a methyl-chloroform-optimized,
257 inter-annually repeating OH field. The inversion propagates uncertainty estimates from the
258 measurements, model and prior emissions growth rate to derive *a posteriori* emissions
259 uncertainty. In this work, the prior emissions growth rate uncertainty was somewhat arbitrarily
260 chosen at a level of 20% of the maximum *a priori* emissions. In contrast to Rigby et al. (2014),
261 in which a scaling factor of the emissions was solved for in the inversion, here we determined
262 absolute emissions, which were found to lead to more robust uncertainty estimates when
263 emissions were very low. *A posteriori* emissions uncertainties were augmented with an estimate
264 of the influence of uncertainties in the lifetime, as described in Rigby et al. (2014).

265

266 3. Results and Discussion

267 3.1. Atmospheric mole fractions

268 Figure 1 shows the HFC-23 modelled mole fraction for the four equal-mass latitudinal
269 subdivisions of the global atmosphere calculated from the 12-box model and the combined GC-
270 MS-Medusa *in situ* measurements (2008-2016), firm air data and CGAA data. The lower box
271 shows the annual growth rates in $\text{pmol mol}^{-1} \text{yr}^{-1}$. We find that the global modelled annual mole
272 fraction of HFC-23 in the background atmosphere reached $28.9 \pm 0.6 \text{ pmol mol}^{-1}$, (1σ confidence
273 interval) in December 2016, a 163% increase from 1995 and a 28% increase from the 22.6 ± 0.2
274 pmol mol^{-1} reported in 2009 (Miller et al, 2010). In 2008 the annual mean mid-year growth rate
275 of HFC-23 was $0.78 \text{ pmol mol}^{-1} \text{yr}^{-1}$. The rate of accumulation then decreased in mid-2009 to
276 $0.68 \text{ pmol mol}^{-1} \text{yr}^{-1}$, rising to a maximum of $1.05 \text{ pmol mol}^{-1} \text{yr}^{-1}$ in early 2014, followed by a
277 smaller decrease to $0.95 \text{ pmol mol}^{-1} \text{yr}^{-1}$ at the end of 2016. The rate of accumulation of HFC-23
278 increased by 22 % from 2008 to 2016. In the Figure 1 inset, we compare the annual mean mole
279 fractions of HFC-23 and HCFC-22 recorded at Mace Head and Cape Grim, as examples of a



280 mid-latitude northern hemisphere (NH) and southern hemisphere (SH) site, which illustrates the
281 divergence between these two compounds at both sites beginning around 2010.

282 Figure 2 shows our HCFC-22 modelled mole fractions for the four equal-mass latitudinal
283 subdivisions of the global atmosphere calculated from the 12-box model and the lower box
284 shows the HCFC-22 annual growth rates in $\text{pmol mol}^{-1} \text{yr}^{-1}$. The global modelled HCFC-22
285 annual mixing ratio in the background atmosphere reached a peak of $238 \pm 2 \text{ pmol mol}^{-1}$ in
286 December 2016, noting also that the annual average global growth rate of HCFC-22 decelerated
287 from 2008 to 2016 at an annual average rate of $0.5 \text{ pmol mol}^{-1} \text{yr}^{-2}$. This decline in the global rate
288 of accumulation of HCFC-22 coincides with the phase out of HCFCs mandated by the 2007
289 adjustment to the MP for Annex 1 countries, covering dispersive applications, but not the non-
290 dispersive use of HCFC-22 as a feedstock in fluoropolymer manufacture (UNEP, 2007).
291 Nevertheless, HCFC-22 remains the dominant HCFC in the atmosphere and accounts for 79%
292 by mass of the total global HCFC emissions, (Simmonds et al., 2017). In contrast to the
293 increasing growth rate of HFC-23, the growth rate of HCFC-22 has exhibited a steep 53%
294 decline from a maximum in January 2008 of $8.2 \text{ pmol mol}^{-1} \text{yr}^{-1}$ to $3.8 \text{ pmol mol}^{-1} \text{yr}^{-1}$ in
295 December 2016, further illustrating the divergence between these two gases between 2008 and
296 2016 (compare lower boxes in Figures 1 and 2).

297 3.2. Global emission estimates

298 Miller et al., (2010) calculated global emissions of HFC-23 using the same AGAGE 12-
299 box model as used here, but with a different Bayesian inverse modelling framework. Following a
300 peak in emissions in 2006 of $15.9 (+1.3/-1.2) \text{ Gg yr}^{-1}$, modelled emission estimates of HFC-23
301 declined rapidly to $8.6 (+0.9/-1.0) \text{ Gg yr}^{-1}$ in 2009, which Miller noted was the lowest annual
302 emission for the previous 15 years. Based on the analysis of firm air samples and ambient air
303 measurements from Antarctica, Montzka et al. (2010) reported global HFC-23 emissions of 13.5
304 $\pm 2 \text{ Gg yr}^{-1}$ ($200 \pm 30 \text{ Mt CO}_2\text{-eq. yr}^{-1}$), averaged over 2006-2008. In Carpenter and Reimann
305 (2014), global emissions of HFC-23 estimated from measured and derived atmospheric trends
306 reached a maximum of 15 Gg yr^{-1} in 2006, fell back to 8.6 Gg yr^{-1} in 2009, and subsequently
307 increased again to 12.8 Gg yr^{-1} in 2012 (Figure 1-25, update of Miller et al., 2010 and Montzka et al.,
308 2010).

309 The model derived HFC-23 emissions from this study, shown in Figure 3 and listed in
310 Table 2, reached an initial maximum in 2006 of $13.3 \pm 0.8 \text{ Gg yr}^{-1}$, then declined steeply to $9.6 \pm$
311 0.6 Gg yr^{-1} in 2009, in accord with the HFC-23 global emissions estimates of Miller et al.,
312 (2010) and Carpenter and Reimann (2014). Our mean annual (2006-2008) HFC-23 emissions
313 of $12.1 (\pm 0.7) \text{ Gg yr}^{-1}$ are lower than the Montzka et al., (2010) emissions, but agree within



314 uncertainties. However, our HFC-23 emissions then grew rapidly reaching a new maximum of
315 $14.5 \pm 0.6 \text{ Gg yr}^{-1}$ ($180 \pm 7 \text{ Mt CO}_2\text{-eq. yr}^{-1}$) in 2014, only to decline again to $12.7 \pm 0.6 \text{ Gg yr}^{-1}$
316 ($157 \pm 7 \text{ Mt CO}_2\text{-eq. yr}^{-1}$) in 2016.

317 The global emission estimates for HCFC-22 are plotted in Figure 4 together with the
318 corresponding Miller et al., (2010) emissions up to 2008 and the WMO 2014 emissions
319 estimates (Carpenter and Reimann, 2014). Table 3 lists the global emission estimates, mole
320 fractions and growth rate of HCFC-22. Our modelled HCFC-22 emissions reached a maximum
321 global emission of $385 \pm 41 \text{ Gg yr}^{-1}$ ($696 \pm 74 \text{ Mt CO}_2\text{-eq. yr}^{-1}$) in 2010, followed by a slight
322 decline to $370 \pm 46 \text{ Gg yr}^{-1}$ ($670 \pm 83 \text{ Mt CO}_2\text{-eq. yr}^{-1}$) in 2016 at an annual average rate of 2.3
323 Gg yr^{-1} .

324 3.2. Regional emissions

325 There are a significant number of papers which report Asian emissions of HFC-23, including
326 those for China (Yokouchi et al., 2006; Stohl et al., 2010; Kim et al., 2010; Li et al., 2011; Yao
327 et al., 2012). Recent papers by Fang et al. (2014, 2015) noted some inconsistencies between the
328 various bottom-up and top-down emissions estimates in these reports and provided an improved
329 bottom-up inventory and a multiannual top-down estimate of HFC-23 emissions for East Asia.
330 They further demonstrated that China contributed 94-98 % of all HFC-23 emissions in East Asia
331 and was the dominant contributor to global emissions $20 \pm 6 \%$ in 2000 rising to $77 \pm 23 \%$ in
332 2005. China's annual HFC-23 top-down emissions in 2012 were estimated at $8.8 \pm 0.8 \text{ Gg yr}^{-1}$
333 (Fang et al., 2015) which represents 69% of our 2012 global emissions estimate of $12.9 \pm 0.6 \text{ Gg}$
334 yr^{-1} , listed in Table 2.

335 Based on the bottom-up estimated global HFC-23 emissions (shown in Supplementary
336 Material (1), Table S2), we plot in Figure 5a absolute global and Chinese emissions and the
337 percentage of Chinese emissions contributing to the global total. These bottom-up estimates
338 show that a steadily increasing quantity of global total HFC-23 emissions can be attributed to
339 China, averaging about 88% in 2011-2014. This rise is consistent with our calculated bottom-up
340 HCFC-22 production data compiled from industry sources and listed in Supplementary Material
341 (1), Table S1. Figure 5b, shows the bottom-up estimates of global and China HCFC-22
342 production and the percentage contribution of China production to the global total, further
343 illustrating the dominance of Chinese HCFC-22 production.

344 Clearly China is the major contributor to recent global HFC-23 emissions which implies only
345 minor contributions from other regional emitters. Because HFC-23 pollution events are still
346 observed at our European sites, we examine the contribution from European emissions, using a



347 similar methodology as reported by Keller et al., (2011). In this study we compute surface source
348 sensitivities for the AGAGE sites at Jungfraujoch and Mace Head with a Lagrangian Particle
349 Dispersion Model (LPDM) FLEXPART (Stohl et al., 2005) and a spatially resolved, regional-
350 scale emission inversion, using the FLEXPART-derived source sensitivities and a Bayesian
351 approach (Brunner et al., 2017; Henne et al., 2016) to estimate European HFC-23 emissions for
352 the years 2009 to 2016. Two different approaches were used to spatially distribute *a priori*
353 emissions generated from individual national inventory reports to UNFCCC in 2017. The key
354 results from this work are shown in Figure 6 and in Table 4 and full details are available in the
355 Supplementary Material (3).

356 Based on these inversion results, European emissions of HFC-23, though small on a
357 global scale were, in general, larger than reported to UNFCCC and exhibited considerable year-
358 to-year variability. Total *a posteriori* emissions for the six regions listed in Table 4 reached a
359 maximum of $296 \pm 46 \text{ Mg yr}^{-1}$ in 2013 declining to $169 \pm 30 \text{ Mg yr}^{-1}$ in 2016 and showed a
360 slightly negative, statistically insignificant trend over the period analysed (2009-2016). The
361 cumulative European HFC-23 emissions from 2010-2016 were $\sim 1.3 \text{ Gg}$ corresponding to just
362 1.5% of our cumulative global HFC-23 emissions over this same period of 89 Gg, (listed in
363 Table 2). Considerable differences between the two inversions with different *a priori* emission
364 distributions occurred on the country scale, with generally larger Italian *a posteriori* emissions
365 when the original UNFCCC split of point and area sources was used in the *a priori*. In this case
366 the inversion was not able to completely relocate the area emissions, but at the same time
367 increased emissions at the point source locations and resulting in overall larger *a posteriori*
368 emissions.

369 In the following section we attempt to reconcile the changing trends in global HFC-23
370 emissions with the decrease in global HCFC-22 emissions after 2010 and the decline in the
371 annual HCFC-22 growth rate. There are a number of key factors which we believe can explain
372 the changing trend in the recent history of HFC-23 emissions after the minimum in 2009. We
373 also note that this minimum occurred during the global financial crisis of 2007-2009 and in fact
374 HFC-23 emissions mirror global GDP growth rates for the years before and after 2009
375 (<https://data.worldbank.org/indicator.NY.GDP.MKTP.CD>). We can only speculate that this may
376 have reduced the overall demand for PTFE, thereby impacting global HCFC-22 production and
377 the co-produced HFC-23.

378



379 3.3. Factors affecting the recent increase in HFC-23 emissions and changes in the
380 consumption of produced HCFC-22.

381 1. Recent publications have highlighted the substantial increase in HCFC-22 production in
382 Non-Annex 1 countries since the 1990s, especially in the last decade, due to increasing demand
383 in air-conditioning, refrigeration and primarily from the use of HCFC-22 as a feedstock in
384 fluoropolymer manufacture (UNEP, 2009; Miller et al., 2010; Fang et al., 2015; USEPA, 2013).
385 This has resulted in Non-Annex 1 countries emitting more co-produced HFC-23 than Annex 1
386 countries since about 2001 (Miller et al., 2010). HCFC-22 production in Annex 1 countries in
387 2015 had shrunk by 45% from the peak historic value of 407 Gg yr⁻¹ in 1996 (see
388 Supplementary Material (1), Table S1). This has been accomplished by plant closures and
389 further reductions of HFC-23 emissions have been achieved by enhanced destruction in the
390 remaining plants. Nevertheless, ~ 1Gg of HFC-23 were emitted in 2015 from HCFC-22
391 production in Annex 1 countries, mainly from Russia and USA (96%). For comparison, the
392 combined HFC-23 emissions in 2015 from the six European regions (listed in Table 4) were just
393 0.1 ± 0.03 Gg.

394
395 2. Since 2006, a major factor mitigating HFC-23 emissions has been the CERs issued under
396 the CDM. However, under the original CDM rules, large CERs that cost relatively little to
397 acquire could be claimed legitimately (Munnings et al., 2016) and the rules were changed to bar
398 new entrants to the mechanism after 2009. The HFC-23/HCFC-22 co-production or waste gas
399 generation ratio varies between 1.5-4% (by mass) depending on HCFC-22 plant operating
400 conditions and process optimization (McCulloch and Lindley, 2007). Under the
401 UNFCCC/CDM, 19 HCFC-22 production plants in five Non-Annex 1 countries - Argentina (1),
402 China (11), Democratic People's Republic of Korea (1), India (5), and Mexico (1) - were
403 approved for participation in CDM projects. These countries reportedly incinerated 5.7 Gg and
404 6.8 Gg of HFC-23 in 2007 and 2008, respectively (UNFCCC, 2009). This represented 43-48%
405 of the HCFC-22 produced in Non-Annex 1 countries during 2007-2008 assuming the 1.5 - 4%
406 co-production factor (Montzka et al., 2010). These same five countries produced 597 Gg of
407 HCFC-22 from controlled and feed stock uses in 2015. HFC-23 generated from this HCFC-22
408 production was estimated at 16 Gg with an average co-production ratio of 2.6%. Furthermore, it
409 was estimated that China produced 535 Gg of HCFC-22 in 2015 (~90% of the five countries'
410 total production) and 45% of the co-produced HFC-23 generated was destroyed in the CDM
411 destruction facilities (UNEP, 2017a). We also acknowledge that the first seven-year crediting
412 period of CDM projects in China expired in 2013, concurrent with the European Union ceasing
413 the purchase of CER credits produced in industrial processes after May 2013 (Fang et al., 2014).



414 3. Lastly, we should consider whether there are other sources of HFC-23 which might
415 explain an increase in global emissions. While the source of all HFC-23 is HCFC-22 co-
416 production, material that is recovered and sold may subsequently be emitted to the atmosphere.
417 Emissions of HFC-23 from fire suppression systems are negligible relative to global production
418 (McCulloch and Lindley, 2007) and emissions from all emissive uses are reported to be 133 ± 9
419 Mg yr^{-1} from Annex 1 countries (UNFCCC, 2017) and less than 2.5 Mg for the refrigeration and
420 firefighting sectors in 2015 in the five Non-Annex 1 countries listed above, (UNEP, 2017a).
421 Semi-conductor use of HFC-23 is insignificant having been replaced by more efficient etchants
422 and where destruction efficiencies are greater than 90% (Bartos et al., 2006, Miller et al., 2010).
423 Fraser et al., (2013) reported a very small emissions factor of $0.04 \text{ g HFC-23 Mg}^{-1}$ aluminium
424 (Al) from the Kurri Kurri smelter plant in NSW, Australia. It was estimated that this corresponds
425 to an annual emission of HFC-23 from Al production of $\sim 3 \text{ Mg}$ based on a global Al production
426 of 57 Tg in 2016. Realistically, these other potential industrial sources of HFC-23 emissions are
427 very small ($<140 \text{ Mg yr}^{-1}$) in the context of global emissions estimates.

428 The combination of these factors strongly suggests that the steep reversal of the
429 downwards trend in HFC-23 emissions after 2009 is attributable to HFC-23 abatement measures
430 not being adequate to offset the increasing growth of HCFC-22 for non-dispersive feedstock.
431 This is despite the initial success of CDM abatement technologies leading to mitigation of HFC-
432 23 emissions during 2006-2009.

433

434 4. Conclusions

435 As noted above, the introduction of CERs under the CDM did contribute to a reduction
436 of HFC-23 emissions in Non-Annex 1 countries during 2006-2009, thereby lowering global
437 emissions which reached a minimum in 2009 of $9.6 \pm 0.6 \text{ Gg yr}^{-1}$. However, from 2010 to 2014
438 global HFC-23 emissions increased steadily at an annual average rate of $\sim 1 \text{ Gg yr}^{-1}$ reaching a
439 new maximum in 2014 of $14.5 \pm 0.6 \text{ Gg yr}^{-1}$. This period coincides with the highest levels of
440 our bottom-up estimates of HCFC-22 production in Non-Annex 1 countries (Supplementary
441 Material (1), Table S1), and appears to be in a transition period when HCFC-22 production
442 plants without any abatement controls had yet to install incineration technologies, or fully adopt
443 process optimisation techniques. Furthermore, non-CDM plants are not required to report co-
444 produced HFC-23 emissions, although Fang et al. (2015) calculated that these plants have a
445 lower HFC-23/HCFC-22 production ratio as they came into operation after the CDM plants and
446 would most likely be using improved technologies for HFC-23 abatement.



447 Our cumulative HFC-23 emissions estimates from 2010 to 2016 were 89.1 Gg (1.1 ± 0.2
448 Gt CO₂-eq), which led to an increase in radiative forcing of 1.0 ± 0.1 mW m⁻². This implies that
449 the post-2009 increase in HFC-23 emissions represents a consequence of the decision not to
450 award new CDM projects after 2009, against a background of increasing production of HCFC-
451 22 in plants that did not have abatement technology. Over this same time frame, the magnitude
452 of the cumulative emissions of HCFC-22 was 2610 Gg (4724 Mt CO₂-eq. yr⁻¹). During 2015-
453 2016 our results show a decline of about 9 % in average global HFC-23 emissions (12.9 Gg yr⁻¹)
454 relative to the 2013-2014 average of 14.2 Gg yr⁻¹. We note that in the Kigali 2016 Amendment
455 to the MP, China was subject to domestic dispersive HCFC-22 production reduction of 10% by
456 2015 compared to the average 2009-2010 production (UNEP, 2017a). While this regulation
457 should decrease HCFC-22 production for dispersive uses, overall HFC-23 emissions could still
458 continue to increase due to a potential increase in the production of HCFC-22 for feedstock uses,
459 (Fang et al., 2014). It is perhaps encouraging that the Kigali Amendment also stipulates that the
460 Parties to the MP shall ensure that HFC-23 emissions generated from production facilities
461 producing HCFCs or HFCs are destroyed to the extent possible using technology yet to be
462 approved by the Parties. With the support of the Chinese Government, 13 new destruction
463 facilities at 15 HCFC-22 production lines not covered by CDM were started in 2014 (UNEP,
464 2017a). The timing of these new initiatives is consistent with the most recent reduction (2015-
465 2016) of global HFC-23 emissions, although we cannot confirm a direct link.

466

467 The mismatch between mitigation and emissions, that is most evident in China, suggests
468 that the delay in the implementation of additional abatement measures allowed HFC-23
469 emissions to increase before these measures became effective. Our results imply that un-abated
470 HFC-23 emissions will continue to be released into the atmosphere and will continue to make a
471 contribution to radiative forcing of HFCs until the implementation of abatement becomes a
472 universal requirement.

473

474

475

476

477

478

479

480

481

482 **Acknowledgements**

483 We specifically acknowledge the cooperation and efforts of the station operators (G.
484 Spain, Mace Head, Ireland; R. Dickau, Trinidad Head, California; P. Sealy, Ragged Point,
485 Barbados; NOAA Officer-in-Charge, Cape Matatula, American Samoa; S. Cleland, Cape Grim,
486 Tasmania) and their staff at all the AGAGE stations. The operation of the AGAGE stations was
487 supported by the National Aeronautics and Space Administration (NASA, USA) (grants NAG5-
488 12669, NNX07AE89G, NNX11AF17G and NNX16AC98G to MIT; grants NAG5-4023,
489 NNX07AE87G, NNX07AF09G, NNX11AF15G, NNX11AF16G, NNX16AC96G and
490 NNX16A97G to SIO). Also through the Department for Business, Energy & Industrial Strategy
491 (BEIS, UK, formerly the Department of Energy and Climate Change (DECC)) contract
492 1028/06/2015 to the University of Bristol and the UK Meteorological Office for Mace Head,
493 Ireland; the National Oceanic and Atmospheric Administration (NOAA, USA), contract RA-
494 133-R15-CN-0008 to the University of Bristol for Ragged Point, Barbados in addition to the
495 operations of the American Samoa station, by the Commonwealth Scientific and Industrial
496 Research Organisation (CSIRO, Australia), the Bureau of Meteorology (Australia) and
497 Refrigerant Reclaim Australia.

498 M. Rigby is supported by a NERC Advanced Fellowship NE/I021365/1. We
499 acknowledge the cooperation of R. Langenfelds for his long-term involvement in supporting and
500 maintaining the Cape Grim Air Archive. We also thank S. Montzka and B. Hall for supplying
501 actual datasets from their publications.

502

503

504

505

506

507

508

509

510

511

512 **References.**

- 513 | Arnold, T., Mühle, J., Salameh, P. K., Harth, C.M., Ivy, D. J., and Weiss, R. F.: Automated
514 measurement of nitrogen trifluoride in ambient air, *Anal. Chem.*, 84, 4798–4804, 2012.
- 515 Bartos S., Beu, L. S., Burton, C. S., Fraust, C. L., Illuzzi, F., Mocella, M. T., and Raoux, S.: IPCC
516 Guidelines for National Greenhouse Inventories. Volume 3, Industrial Processes, Chapter 6,
517 Electronics Industry, available on line at: [www.ipcc-nggip.iges.or.jp/public/2006gl/pdf/3_Volume3/V3.6.Ch6_Electronics_Industry](http://www.ipcc-nggip.iges.or.jp/public/2006gl/pdf/3_Volume3/V3.6.Ch6_Electronics_Industry.pdf), pdf, 2006.
- 519 Brunner, D., Arnold, T., Henne, S., Manning, A., Thompson, R. L., Maione, M., O'Doherty, S.,
520 and Reimann, S.: Comparison of four inverse modelling systems applied to the estimation of
521 HFC-125, HFC-134a and SF₆ emissions over Europe, *Atmos. Chem. Phys.*, 17, 10651-10674,
522 <https://doi.org/10.5194/acp-17-10674-2017>, 2017.
- 523 Burkholder, J. B., Sander, S. P., Abbatt, J., Barker, R., Huie, R. E., Kolb, C. E., Kurylo, M. J.,
524 Orkin, V. L., Wilmouth, D. M., and Wine, P.H.: Chemical kinetics and photochemical data for
525 use in atmospheric studies, Evaluation No. 18, JPL Publication 15-10, Jet Propul. Lab.,
526 Pasadena, Calif, 2015. [available at <http://jpldataeval.jpl.nasa.gov>.]
- 527 Buizert, C., Martinerie, P., Petrenko, V. V., Severinghaus, J. P., Trudinger, C. M., Witrant, E.,
528 Rosen, J. L., Orsi, A. J., Rubino, M., Etheridge, D. M., Steele, L. P., Hogan, C., Laube, J. C.,
529 Sturges, W. T., Levchenko, V. A., Smith, A. M., Levin, I., Conway, T. J., Dlugokencky, E. J.,
530 Lang, P. M., Kawamura, K., Jenk, T. M., White, J. W. C., Sowers, T., Schwander, J., and
531 Blunier, T.: Gas transport in firn: multiple-tracer characterisation and model intercomparison for
532 NEEM, Northern Greenland, *Atmos. Chem. Phys.*, 12, 4259–4277, doi:10.5194/acp-12-4259-
533 2012.
- 534 Butler, J. H., Montzka, S. A., Battle, M., Clarke, A. D., Mondeel, D. J., Lind, J. A., Hall, B. D.,
535 and Elkins, J. W.: Collection and Analysis of Firn Air from the South Pole, 2001, AGU Fall
536 Meeting Abstracts, p. F145, 2001.
- 537 Carpenter, L. J. and Reimann, S.: Ozone-Depleting Substances (ODSs) and Other Gases of
538 Interest to the Montreal Protocol, Chapter 1, in: Scientific Assessment of Ozone Depletion:
539 2014, Global Ozone Research and Monitoring Project - Report No. 55, World Meteorological
540 Organisation, Geneva, Switzerland, 2014.
- 541 Cunnold, D. M., Alyea, F. N., Prinn, R.G.: A Methodology for Determining the Atmospheric
542 Lifetime of Fluorocarbons, *J. Geophys. Res.*, 83, 5493-5500, 1978.
- 543 Cunnold, D. M., Prinn, R.G., Rasmussen, R., Simmonds, P. G., Alyea, F. N., Cardlino, C.,
544 Crawford, A. J., Fraser, P. J., Rosen, R.: The Atmospheric Lifetime Experiment, III: lifetime
545 methodology and application to three years of CFC₁₃ data, *J. Geophys. Res.*, 88, 8379-8400,
546 1983.
- 547 Cunnold, D. M., Fraser, P. J., Weiss, R. F., Prinn, R. G., Simmonds, P. G., Miller, B. R., Alyea,
548 F. N., Crawford, A. J., and Rosen, R.: Global trends and annual releases of CCl₃F and CCl₂F₂
549 estimated from ALE/GAGE and other measurements from July 1978 to June 1991, *J. Geophys.*
550 *Res.*, 99, 1107-1126, 1994.



- 551 Fang, X., Miller, B. R., Su, S., Wu, J., Zhang, J., and Hu, J.: Historical emissions of HFC-23
552 (CHF₃) in China and projections upon policy options by 2050. *Environ. Sci. & Technol.*, 48,
553 4056-4062, 2014.
- 554 Fang, X., Stohl, A., Yokouchi, Y., Kim, J., Li, S., Saito, T., Park S and Hu, J.: Multiannual top-
555 down estimate of HFC-23 emissions in East Asia. *Environ. Sci. & Technol.*, 49, 4345-4353,
556 2015.
- 557 Fraser, P. J., Langenfelds, R.L., Derek N and Porter, L.W.: Studies in air archiving techniques,
558 in *Baseline Atmospheric Program (Australia) 1989*, S. R. Wilson and J. L. Gras (eds.),
559 Department of the Arts, Sport, the Environment, Tourism and Territories, Bureau of
560 Meteorology and CSIRO Division of Atmospheric Research, Canberra, Australia, 16-29, 1991.
- 561 Fraser, P., Steele, L.P., and Cooksey, M.: PFC and carbon dioxide emissions from an Australian
562 aluminium smelter using time-integrated stack sampling and GC-MS, GC-FID analysis. *Light*
563 *Metals 2013*, B. Sadler (ed.), Wiley/TMS 2013, 871-876, 2013.
- 564 Fraser, P. J., Steele, L.P., Pearman, G.I., Coram, S., Derek, N., Langenfelds, R.L and Krummel,
565 P.B.: Non-carbon dioxide greenhouse gases at Cape Grim: a 40 year odyssey, *Baseline*
566 *Atmospheric Program (Australia) History and Recollections, 40th Anniversary Special Edition*,
567 Derek, N., P. B. Krummel and S. J. Cleland (eds.), Bureau of Meteorology/CSIRO Oceans and
568 Atmosphere, ISSN 0155-6959, 45-76, 2016 (November 2016).
- 569 Fuller, E. N., Schettler, P. D., and Giddings, J. C.: A new method for prediction of binary gas-
570 phase diffusion coefficients, *Ind. Eng. Chem.*, 30, 19–27, 1966.
- 571 Hall, B.D., Engel, A., Mühle, J., Elkins, J. W., Artuso, F., Atlas, E., Aydin, M., Blake, D.,
572 Brunke, E.-G., Chiavarini, S., Fraser, P. J., Happell, J., Krummel, P. B., Levin, I., Loewenstein,
573 M., Maione, M., Montzka, S. A., O'Doherty, S., Reimann, S., Rhoderick, G., Saltzman, E. S.,
574 Scheel, H. E., Steele, L. P., Vollmer, M. K., Weiss, R. F., Worthy, D., and Yokouchi, Y. 2014.:
575 Results from the International Halocarbons in Air Comparison Experiment (IHALACE), *Atmos.*
576 *Meas. Tech.*, 72, 469-490. doi:10.5194/amt-7-469-2014.
- 577 Harrison, J. J., Boone, C. D., Brown, A. T., Allen, N. D. C., Toon, G. C., and Bernath, P. F.:
578 First remote sensing observations of trifluoromethane (HFC-23) in the upper troposphere and
579 lower stratosphere, *J. Geophys. Res.*, 117, D05308, doi: 10.1029/2011JD016423, 2012.
- 580 Henne, S., Brunner, D., Oney, B., Leuenberger, M., Eugster, W., Bamberger, I., Meinhardt, F.,
581 Steinbacher, M., and Emmenegger, L.: Validation of the Swiss methane emission inventory by
582 atmospheric observations and inverse modelling, *Atmos. Chem. Phys.*, 16, 3683-3710, doi:
583 10.5194/acp-16-3683-2016, 2016.
- 584 Keller, C. A., Brunner, D., Henne, S., Vollmer, M. K., O'Doherty, S., and Reimann, S.:
585 Evidence for under-reported western European emissions of the potent greenhouse gas HFC-23.
586 *Geophys. Res. Lett.*, 38, L15808, doi: 10.1029/2011GL047976, 2011.
- 587 Kim, J., Li, S., Kim, K. R., Stohl, A., Mühle, J., Kim, S. K., Park, M. K., Kang, D. J., Lee, G.,
588 Harth, C. M., Salameh, P. K., and Weiss, R. F.: Regional atmospheric emissions determined
589 from measurements at Jeju Island, Korea: Halogenated compounds from China. *Geophys. Res.*
590 *Lett.*, 37, doi:10.1029/2010GL043263, 2010.



- 591 Langenfelds, R. L., Fraser, P. J., Francey, R. J., Steele, L. P., Porter, L. W., Allison, C. E.: The
592 Cape Grim Air Archive: The first seventeen years, 1978-1995. In: Baseline Atmospheric
593 Program Australia 1994-95, edited by R.J. Francey, A.L. Dick and N. Derek, Bureau of
594 Meteorology and CSIRO Division of Atmospheric Research, Melbourne, Australia, pp. 53-70,
595 1996.
- 596 Langenfelds, R., Fraser, P.J., Steele, L.P., and Porter, L.W.: Archiving of Cape Grim air, paper
597 presented at Baseline Atmospheric Program (Australia), Bureau of Meteorology and CSIRO
598 Division of Atmospheric Research, Melbourne, 2003.
- 599 Li, S.; Kim, J.; Kim, K. R.; Mühle, J.; Kim, S. K.; Park, M. K.; Stohl, A.; Kang, D. J.; Arnold,
600 T.; Harth, C. M.; Salameh, P. K.; Weiss, R. F.: Emissions of halogenated compounds in East
601 Asia determined from measurements at Jeju Island, Korea. *Environ. Sci. Technol.*, 45 (13),
602 5668–5675, 2011.
- 603 McCulloch, A.: Incineration of HFC-23 Waste Streams for Abatement of Emissions from
604 HCFC-22 Production: A Review of Scientific, Technical and Economic Aspects, commissioned
605 by the UNFCCC secretariat to facilitate the work of the Methodologies Panel of the CDM
606 Executive Board, available online at: [http://cdm.unfccc.int/methodologies/Background](http://cdm.unfccc.int/methodologies/Background240305.pdf)
607 240305.pdf, 2004.
- 608 McCulloch, A., Lindley, A. A.: Global Emissions of HFC-23 estimated to year 2015. *Atmos.*
609 *Environ*, 41, 1560-1566, 2007.
- 610 Miller, B. R., Weiss, R. F., Salameh, P. K., Tanhua, T., Grealley, B. R., Mühle, J., Simmonds, P,
611 G.: Medusa: A sample pre-concentration and GC-MS detector system for *in situ* measurements
612 of atmospheric trace halocarbons, hydrocarbons and sulphur compounds, *Anal. Chem.*, 80,
613 1536-1545, 2008.
- 614 Miller, B. R., Rigby, M., Kuijpers, L. J. M., Krummel, P. B., Steele, L. P., Leist, M., Fraser, P.
615 J., McCulloch, A., Harth, C. M., Salameh, P.K., Mühle, J., Weiss, R. F., Prinn, R.G., Wang, R.
616 H. J., O'Doherty, S., Grealley, B. R., and Simmonds, P. G.: HFC-23 (CHF₃) emission trend
617 response to HCFC-22 (CHClF₂) production and recent HFC-23 emissions abatement measures,
618 *Atmos. Chem. Phys.*, 10, 7875-7890, 2010.
- 619 Miller, B. R., and Kuijpers, L. J. M.: Projecting future HFC-23 emissions. *Atmos. Chem. Phys.*,
620 11, 13259-13267, doi:10.5194/acp-11-13259-2011, 2011
- 621 Miller, M., and Batchelor, T.: Information paper on feedstock uses of ozone-depleting
622 substances, 72 pp. [Available at [http://ec.europa.](http://ec.europa.eu/clima/policies/ozone/research/docs/feedstock_en.pdf)
623 [eu/clima/policies/ozone/research/docs/feedstock_en.pdf](http://ec.europa.eu/clima/policies/ozone/research/docs/feedstock_en.pdf).] 2012.
- 624 Montzka, S.A., Kuijpers, L., Battle, M. O., Aydin, M., K. R., Vverhulst, K. R., Saltzman, E.S.
625 and Fahey, D. W., Recent increases in global HFC-23 emissions, *Geophys. Res. Lett.*, 37,
626 L02808, doi:10.1029/2009GL041195, 2010..
- 627 Mühle, J., Ganesan, A. L., Miller, B. R., Salameh, P. K., Harth, C. M., Grealley, B. R., Rigby, M.,
628 Porter, L. W., Steele, L. P., Trudinger, C. M., Krummel, P. B., O'Doherty, S., Fraser, P. J.,
629 Simmonds, P. G., Prinn, R. G., Weiss, R. F.: Perfluorocarbons in the global atmosphere:



- 630 tetrafluoromethane, hexafluoroethane, and octafluoropropane. Atmos. Chem. Phys., 10, 5145–
631 5164, doi:10.5194/acp-10-5145, 2010.
- 632 Munnings, C., Leard, B., and Bento, A.: The net emissions impact of HFC-23 offset projects
633 from the Clean Development Mechanism. Resources for the Future, Discussion Paper 16-01,
634 2016.
- 635 Myhre, G., Shindell, D., Bréon, F. M., Collins, W., Fuglestedt, J., Huang, J., Koch, D.,
636 Lamarque, J. F., Lee, D., Mendoza, B., Nakajima, T., Robock, A., Stephens, G., Takemura, T.,
637 and Zhang, H.: Anthropogenic and Natural Radiative Forcing. In: Climate Change 2013: The
638 Physical Science Basis. Contribution of Working Group I to the Fifth Assessment Report of the
639 Intergovernmental Panel on Climate Change [Stocker, T.F., D. Qin, G.-K. Plattner, M. Tignor,
640 S.K. Allen, J. Boschung, A. Nauels, Y. Xia, V. Bex and P.M. Midgley (eds.)]. Cambridge
641 University Press, Cambridge, United Kingdom and New York, NY, USA, 2013.
- 642 O’Doherty, S., Cunnold, D., Sturrock, G. A., Ryall, D., Derwent, R. G., Wang, R. H. J.,
643 Simmonds, P. G., Fraser, P. J., Weiss, R. F., Salameh, P. K., Miller, B. R., Prinn, R. G.: *In situ*
644 chloroform measurements at AGAGE atmospheric research stations from 1994 –1998. J.
645 Geophys. Res., 106, No. D17, 20,429-20,444, ISSN: 0747-7309, 2001.
- 646 O’Doherty, S., Cunnold, D. M., Miller, B. R., Mühle, J., McCulloch, A., Simmonds, P. G.,
647 Manning, A. J., Reimann, S., Vollmer, M. K., Grealley, B. R., Prinn, R. G., Fraser, P. J., Steele,
648 P., Krummel, P. B., Dunse, B. L., Porter, L. W., Lunder, C. R., Schmidbauer, N., Hermansen,
649 O., Salameh, P. K., Harth, C. M., Wang, R. H. J., Weiss, R. F.: Global and regional emissions of
650 HFC-125 (CHF₂CF₃) from *in situ* and air archive atmospheric observations at AGAGE and
651 SOGE Observatories. J. Geophys. Res., 114, D23304, 2009.
- 652 Oram, D.E., Sturges, W. T., Penkett, S. A., McCulloch, A., and Fraser, P. J.: Growth of
653 fluoroform (CHF₃, HFC-23) in the background atmosphere. Geophys. Res. Lett, 25, 35-38,
654 1998.
- 655 Prinn, R. G., Weiss, R. F., Fraser, P. J., Simmonds, P. G., Cunnold, D. M., Alyea, F. N.,
656 O’Doherty, S., Salameh, P. K., Miller, B. R., Huang, J., Wang, R. H. J., Hartley, D. E., Harth,
657 C., Steele, L. P., Sturrock, G., Midgley, P. M., McCulloch, A.: A history of chemically and
658 radiatively important gases in air deduced from ALE/GAGE/AGAGE, J. Geophys. Res., 105
659 (D14), 17751-17792, doi: 10.1029/2000JD900141, 2000.
- 660 Rigby, M., Ganesan, A.L., Prinn, R.G.: Deriving emissions time series from sparse atmospheric
661 mole fractions. J. Geophys. Res., 116, D08306, doi:10.1029/2010JD015401, 2011.
- 662 Rigby, M., Prinn, R. G., O’Doherty, S., Montzka, S. A., McCulloch, A., Harth, C. M., Mühle, J.,
663 Salameh, P. K., Weiss, R. F., Young, D., Simmonds, P. G.: Hall, B. D., Dutton, G. S., Nance,
664 D., Mondeel, D. J., Elkins, J. W., Krummel, P. B., Steele, L. P., Fraser, P. J.: Re-evaluation of
665 the lifetimes of the major CFCs and CH₃Cl₃ using atmospheric trends. Atmos. Chem. Phys., 13,
666 1-11, doi:10.5194/acp-13-1-2013, 2013.
- 667
- 668



- 669 Rigby, M., Prinn, R. G., O'Doherty, S., Miller, B. R., Ivy, D., Mühle, J., Harth, C. M., Salameh,
670 P. K., Arnold, T., Weiss, R. F., Krummel, P. B., Steele, P. L., Fraser, P. J., Young, D.,
671 Simmonds, P. G.: Recent and future trends in synthetic greenhouse gas radiative forcing.
672 *Geophys. Res. Lett.*, 41, 2623–2630, 2014.
- 673 Simmonds, P. G., M. Rigby, M., McCulloch, A., O'Doherty, S., Young, D., Mühle, J.,
674 Krummel, P. B., Steele, L. P., Fraser, P. J., Manning, A. J., Weiss, R. F., Salameh, P. K., Harth, C.
675 M., Wang, R. H. J., and Prinn, R. G.: Changing trends and emissions of
676 hydrochlorofluorocarbons (HCFCs) and their hydrofluorocarbons (HFCs) replacements. *Atmos.*
677 *Chem. Phys.* 17, 4641–4655, doi:10.5194/acp-17-4641-2017.
- 678 SPARC Report on the Lifetimes of Stratospheric Ozone-Depleting Substances, Their
679 Replacements, and Related Species, edited by Ko, M., Newman, P., Reimann, S., Strahan, S.,
680 SPARC Report No. 6, WCRP-15/2013, 2013.
- 681 Stohl, A., Forster, C., Frank, A., Seibert, P., and Wotawa, G.: Technical note: The Lagrangian
682 particle dispersion model FLEXPART version 6.2, *Atmos. Chem. Phys.*, 5, 2461–2474, doi:
683 10.5194/acp-5-2461-2005, 2005.
- 684 Stohl, A.; Kim, J.; Li, S.; O'Doherty, S.; Mühle, J.; Salameh, P. K.; Saito, T.; Vollmer, M. K.;
685 Wan, D.; Weiss, R. F.; Yao, B.; Yokouchi, Y.; Zhou, L. X.: Hydrochlorofluorocarbon and
686 hydrofluorocarbon emissions in East Asia determined by inverse modeling. *Atmos. Chem.*
687 *Phys.* 10, 3545–3560, 2010.
- 688 TEAP (Technology and Economic Assessment Panel of the Montreal Protocol), 2006
689 Assessment Report, United Nations Environment Programme, Nairobi, Kenya, 2006.
- 690 Trudinger, C. M., Enting, I. G., Etheridge, D. M., Francey, R. J., Levchenko, V. A., Steele, L. P.,
691 Raynaud, D., and Arnaud, L.: Modeling air movement and bubble trapping in firn, *J. Geophys.*
692 *Res.*, 102, 6747–6763, doi:10.1029/96JD03382, 1997.
- 693 Trudinger, C. M., Etheridge, D. M., Rayner, P. J., Enting, I. G., Sturrock, G. A., and
694 Langenfelds, R. L.: Reconstructing atmospheric histories from measurements of air composition
695 in firn, *J. Geophys. Res.*, 107, 4780, doi:10.1029/2002JD002545, 2002.
- 696 Trudinger, C. M., Enting, I. G., Rayner, P. J., Etheridge, D. M., Buizert, C., Rubino, M.,
697 Krummel, P. B., and Blunier, T.: How well do different tracers constrain the firn diffusivity
698 profile? *Atmos. Chem. Phys.*, 13, doi:10.5194/acp-13-1485-2013, 2013.
- 699 Trudinger, C. M., Fraser, P. J., Etheridge, D. M., Sturges, W. T., Vollmer, M. K., Rigby, M.,
700 Martinierie, P., Mühle, J., Worton, D. R., Krummel, P. B., Steele, L. P., Miller, B. R., Laube,
701 J., Mani, F., Rayner, P. J., Harth, C. M., Witrant, E., Blunier, T., Schwander, J., O'Doherty, S.,
702 and Battle, M.: Atmospheric abundance and global emissions of perfluorocarbons CF₄, C₂F₆ and
703 C₃F₈ since 1800 inferred from ice core, firn, air archive and *in situ* measurements, *Atmos. Chem.*
704 *Phys.*, 16, 11 733–11 754, doi:10.5194/acp-16-11733-2016, 2016.
- 705 UNEP (United Nations Environment Programme), HCFC Production Data,
706 http://ozone.unep.org/Data_Access/, U.N. Environ. Programme. Nairobi, 2009.



- 707 UNEP (2017a), Key aspects related to HFC-23 by-product control technologies
708 UNEP./OzL.Pro/ExCom/78/9. 7 March 2017.
- 709 UNEP (2017b) Production and Consumption of Ozone Depleting Substances under the Montreal
710 Protocol, 1986-2015, United Nations Environment Programme, available at
711 <http://ozone.unep.org/en/data-reporting/data-centre>
- 712 UNFCCC (United Nations Framework Convention on Climate Change), Greenhouse Gas
713 Emissions Data, http://unfccc.int/ghg_data/ghg_data_unfccc/items/4146.php, U.N. Framework
714 Conv. on Climate Change, Bonn, Germany, 2009.
- 715 UNFCCC (2017), Green house Gas Emissions Data, U.N. Framework Conv, on Clim. Change,
716 Bonn, Germany, available at
717 http://unfccc.int/national_reports/annex_i_ghg_inventories/national_inventories_submissions/items/10116.php
718
- 719 USEPA, (2013). Global mitigation of non-CO₂ greenhouse gases: 2010-2030, United States
720 Environmental Protection Agency, September 2013 (EPA-430-R-13-011).
- 721 Vollmer, M. K., Mühle, J., Trudinger, C. M., Rigby, M., Montzka, S. A., Harth, C. M., Miller,
722 B. R., Henne, S., Krummel, P. B., Hall, B. D., Young, D., Kim, J., Arduini, J., Wenger, A., Yao,
723 B., Reimann, S., O'Doherty, S., Maione, M., Etheridge, D. M., Li, S., Verdonik, D. P., Park, S.,
724 Dutton, G., Steele, L. P., Lunder, C. R., Rhee, T. S., Hermansen, O., Schmidbauer, N., Wang, R.
725 H. J., Hill, M., Salameh, P. K., Langenfelds, R. L., Zhou, L., Blunier, T., Schwander, J., Elkins,
726 J. W., Butler, J. H., Simmonds, P. G., Weiss, R. F., Prinn, R. G., and Fraser, P. J.: Atmospheric
727 histories and global emissions of halons H-1211 (CBrClF₂), H-1301 (CBrF₃), and H-2402
728 (CBrF₂CBrF₂), *J. Geophys. Res. Atmos.*, 121, 3663–3686, doi:10.1002/2015JD024488, 2016.
- 729 Vollmer, M. K., Young, D., Trudinger, C.M., Mühle, J., Henne, S., Rigby, M., Park, S., Li, S.,
730 Guillevic, M., Mitrevski, B., Harth, C. M., Miller, B. R., Reimann, S., Yao, B., Steele, L. P.,
731 Wyss, S.A., Hermansen, O., Arduini, J., McCulloch, A., Rhee, T.S., Wang, R. H. J., Salameh, P.
732 K., Lunder, C., Hill, M., Langenfelds, R. L., Ivy, D., O'Doherty, S., Krummel, P. B., Maione,
733 M., Etheridge, D. M., Zhou, L., Fraser, P. J., Prinn, R. G., Simmonds, P. G., and Weiss, R. F.:
734 Atmospheric histories and emissions of chlorofluorocarbons CFC-13 (CClF₃), CFC-114
735 (C₂Cl₂F₄), and CFC-115 (C₂ClF₅), (Submitted) 2017.
736
- 737 Yao, B., Vollmer, M. K., Zhou, L. X., Henne, S., Reimann, S., Li, P. C., Wenger, A., and Hill,
738 M. 2012.: In-situ measurements of atmospheric hydrofluorocarbons (HFCs) and
739 perfluorocarbons (PFCs) at the Shangdianzi regional background station, China. *Atmos. Chem.*
740 *Phys.*, 12, 10181-10193; doi:10.5194/acp-12-10181-2012.
- 741 Yokouchi, Y; Taguchi, S., Saito, T., Tohjima, Y., Tanimoto, H., and Mukai, H.: High frequency
742 measurements of HFCs at a remote site in East Asia and their implications for Chinese
743 emissions. *Geophys. Res. Lett.*, 33, doi:10.1029/2006GL026403, 2006.
- 744
745
746
747
748

749 **Data availability**

750

751 The entire ALE/GAGE/AGAGE data base comprising every calibrated measurement including
 752 pollution events is archived on the Carbon Dioxide Information and Analysis Center (CDIAC) at
 753 the U.S. Department of Energy, Oak Ridge National Laboratory (<http://cdiac.ornl.gov>).

754

755

756

757 Table 1. AGAGE sites used in this study, their coordinates and start date of GC-MS-Medusa
 758 measurements of HFC-23 and HCFC-22.

AGAGE Site	Latitude	Longitude	HFC-23	HCFC-22
Mace Head (MHD), Ireland ¹	53.3° N	9.9° W	Oct. 2007	Nov. 2003
Trinidad Head (THD), California, USA	41.0° N	124.1° W	Sep. 2007	Mar. 2005
Ragged Point (RPB), Barbados	13.2° N	59.4° W	Aug. 2007	May. 2005
Cape Matatula (SMO), American Samoa	14.2° S	170.6° W	Oct. 2007	May. 2006
Cape Grim (CGO), Tasmania, Australia	40.7° S	144.7° E	Nov. 2007	Jan. 2004
Jungfraujoch, Switzerland ¹	46.5°N	8.0°E	Apr. 2008	Aug. 2012
Cape Grim Air Archive			Apr. 1978	Apr. 1978

759 ¹ Observations used for regional European emissions

760

761

762

763

764

765

766

767

768

769

770

771

772



773 Table 2. Annual mean global HFC-23 (CHF₃) emissions, mole fractions, and growth rates,
774 derived from the AGAGE 12-box model.

Year	HFC-23 Global annual emissions (Gg yr ⁻¹) ±1 sigma (σ) Std. Dev.	HFC-23 Global mean mole fraction (pmol mol ⁻¹) ±1 sigma (σ) Std. Dev.	HFC-23 Global growth rate (pmol mol ⁻¹ yr ⁻¹) ±1 sigma (σ) Std. Dev.
1980	4.2 ± 0.7	3.9 ± 0.1	0.33 ± 0.05
1981	4.2 ± 0.8	4.3 ± 0.1	0.33 ± 0.05
1982	4.4 ± 0.7	4.6 ± 0.1	0.35 ± 0.07
1983	5.2 ± 0.7	5.0 ± 0.1	0.41 ± 0.05
1984	5.6 ± 0.7	5.4 ± 0.1	0.44 ± 0.05
1985	5.8 ± 0.8	5.9 ± 0.1	0.45 ± 0.05
1986	5.8 ± 0.7	6.3 ± 0.1	0.45 ± 0.05
1987	5.9 ± 0.7	6.8 ± 0.1	0.46 ± 0.05
1988	6.8 ± 0.7	7.2 ± 0.1	0.52 ± 0.05
1989	7.1 ± 0.7	7.8 ± 0.2	0.55 ± 0.05
1990	7.0 ± 0.7	8.3 ± 0.2	0.54 ± 0.05
1991	7.0 ± 0.7	8.9 ± 0.2	0.54 ± 0.05
1992	7.4 ± 0.6	9.4 ± 0.2	0.57 ± 0.05
1993	7.9 ± 0.6	10.0 ± 0.2	0.61 ± 0.04
1994	8.3 ± 0.7	10.6 ± 0.2	0.64 ± 0.04
1995	8.9 ± 0.6	11.3 ± 0.2	0.69 ± 0.05
1996	9.6 ± 0.6	12.0 ± 0.2	0.74 ± 0.04
1997	10.1 ± 0.6	12.8 ± 0.3	0.77 ± 0.04
1998	10.4 ± 0.7	13.6 ± 0.3	0.79 ± 0.04
1999	10.9 ± 0.7	14.4 ± 0.3	0.82 ± 0.04
2000	10.4 ± 0.8	15.2 ± 0.3	0.76 ± 0.05
2001	9.4 ± 0.7	15.9 ± 0.3	0.68 ± 0.05
2002	9.5 ± 0.7	16.6 ± 0.3	0.69 ± 0.05
2003	10.3 ± 0.8	17.3 ± 0.3	0.77 ± 0.05
2004	11.8 ± 0.8	18.1 ± 0.3	0.90 ± 0.05
2005	13.2 ± 0.8	19.1 ± 0.4	1.01 ± 0.05
2006	13.3 ± 0.8	20.1 ± 0.4	0.99 ± 0.05
2007	11.7 ± 0.7	21.0 ± 0.4	0.85 ± 0.04
2008	11.2 ± 0.6	21.9 ± 0.4	0.78 ± 0.03
2009	9.6 ± 0.6	22.6 ± 0.4	0.68 ± 0.03
2010	10.4 ± 0.6	23.3 ± 0.4	0.74 ± 0.03
2011	11.6 ± 0.6	24.1 ± 0.5	0.85 ± 0.03
2012	12.9 ± 0.6	25.0 ± 0.5	0.96 ± 0.03
2013	14.0 ± 0.6	26.0 ± 0.5	1.04 ± 0.03
2014	14.5 ± 0.6	27.0 ± 0.5	1.05 ± 0.03
2015	13.1 ± 0.7	28.0 ± 0.5	0.95 ± 0.03
2016	12.7 ± 0.6	28.9 ± 0.6	0.94 ± 0.03

775 Note: data are tabulated as annual mean mid-year values.

776 Earlier emissions estimates (1930-1979) determined from the AGAGE 12-box model are
777 listed in Supplementary Material (4), Table S4.

778



779 Table 3. Annual mean global HCFC-22 (CHClF₂) emissions, mole fractions, and growth rates,
 780 derived from the AGAGE 12-box model.

Year	HCFC-22 Global annual emissions (Gg yr ⁻¹) ±1 sigma (σ) Std. Dev.	HCFC-22 Global mean mole fraction (pmol mol ⁻¹) ±1 sigma (σ) Std. Dev.	HCFC-22 Global growth rate (pmol mol ⁻¹ yr ⁻¹) ±1 sigma (σ) Std. Dev.
1980	116.8 ± 17.6	41.6 ± 1.0	4.1 ± 0.9
1981	123.4 ± 18.8	45.8 ± 1.2	4.2 ± 0.8
1982	125.7 ± 15.7	49.9 ± 1.3	4.0 ± 0.8
1983	125.2 ± 20.1	53.7 ± 0.9	3.6 ± 1.0
1984	136.8 ± 18.1	57.3 ± 1.1	4.2 ± 0.6
1985	166.1 ± 17.0	62.2 ± 1.0	5.7 ± 0.7
1986	174.2 ± 19.3	68.5 ± 1.0	5.5 ± 0.7
1987	155.4 ± 20.2	72.9 ± 1.2	4.1 ± 0.7
1988	177.8 ± 19.6	77.2 ± 1.0	5.0 ± 0.7
1989	198.0 ± 19.8	82.9 ± 1.0	6.0 ± 0.7
1990	209.1 ± 19.7	89.1 ± 1.2	6.2 ± 0.6
1991	212.2 ± 21.4	95.1 ± 1.2	5.8 ± 0.7
1992	207.1 ± 23.9	100.5 ± 1.3	5.0 ± 0.6
1993	214.6 ± 22.8	105.4 ± 1.3	5.0 ± 0.6
1994	222.7 ± 22.9	110.4 ± 1.3	5.2 ± 0.5
1995	241.4 ± 26.9	115.9 ± 1.3	5.7 ± 0.5
1996	230.1 ± 24.3	121.4 ± 1.3	4.8 ± 0.5
1997	238.3 ± 24.1	125.8 ± 1.3	5.0 ± 0.5
1998	256.0 ± 27.2	131.7 ± 1.3	5.7 ± 0.4
1999	251.8 ± 28.4	136.8 ± 1.4	5.0 ± 0.3
2000	275.1 ± 28.7	142.0 ± 1.4	5.8 ± 0.2
2001	275.3 ± 28.8	147.9 ± 1.5	5.5 ± 0.2
2002	280.7 ± 31.6	153.1 ± 1.6	5.3 ± 0.2
2003	286.3 ± 30.1	158.3 ± 1.6	5.3 ± 0.2
2004	292.1 ± 30.6	163.7 ± 1.7	5.3 ± 0.2
2005	312.3 ± 34.6	169.2 ± 1.6	6.1 ± 0.2
2006	334.3 ± 35.0	175.9 ± 1.7	7.2 ± 0.2
2007	355.6 ± 35.2	183.6 ± 1.8	8.0 ± 0.2
2008	372.9 ± 38.4	191.9 ± 1.9	7.9 ± 0.2
2009	368.6 ± 39.7	199.2 ± 2.0	7.4 ± 0.2
2010	385.8 ± 41.3	206.8 ± 2.0	7.4 ± 0.3
2011	373.1 ± 41.3	213.7 ± 2.1	6.2 ± 0.2
2012	373.2 ± 45.5	219.3 ± 2.2	5.5 ± 0.2
2013	369.6 ± 44.1	224.7 ± 2.3	5.0 ± 0.2
2014	373.9 ± 45.7	229.5 ± 2.3	4.6 ± 0.2
2015	364.2 ± 47.7	233.7 ± 2.2	3.9 ± 0.2
2016	370.3 ± 45.9	237.5 ± 2.2	3.9 ± 0.2

781 Note: data are tabulated as annual mean mid-year values

782

783

784



785 Table 4: European HFC-23 emissions (t) by country/region: E_a *a priori*, E_b *a posteriori*
 786 emissions, f_a fraction of *a priori* emissions from factory locations, f_b fraction of *a posteriori*
 787 emissions from factory locations. All values represent averages from both inversions using
 788 different *a priori* distributions.

789

year	Germany				France				Italy			
	E_a (Mg/yr)	E_b (Mg/yr)	f_a (%)	f_b (%)	E_a (Mg/yr)	E_b (Mg/yr)	f_a (%)	f_b (%)	E_a (Mg/yr)	E_b (Mg/yr)	f_a (%)	f_b (%)
2009	8±16	34±12	30	49	15±31	2±3.2	88	6	8.4±17	34±8.7	26	52
2010	7.6±15	19±14	27	13	12±23	15±5.1	84	86	9±18	48±9.3	26	45
2011	8±16	44±13	33	58	7.7±15	10±3.4	70	73	9.2±18	34±11	26	43
2012	7.6±15	32±9.7	30	40	8.1±16	8.3±3.4	76	73	9.1±18	25±8.6	26	31
2013	7.2±14	16±9.4	28	58	9.2±18	27±16	82	93	9.3±19	47±24	26	29
2014	7.1±14	20±9.2	30	27	9.4±19	10±2.3	84	85	9.5±19	32±14	26	32
2015	6.6±13	12±8.7	29	14	9.5±19	17±3.9	86	92	9.8±20	37±19	26	24
2016	6.6±13	19±9.1	29	26	9.5±19	9.9±3.4	86	85	9.8±20	23±10	26	39

year	Benelux				United Kingdom				Iberian Peninsula			
	E_a (Mg/yr)	E_b (Mg/yr)	f_a (%)	f_b (%)	E_a (Mg/yr)	E_b (Mg/yr)	f_a (%)	f_b (%)	E_a (Mg/yr)	E_b (Mg/yr)	f_a (%)	f_b (%)
2009	13±27	25±8.8	98	99	3.8±7.6	5.3±3.1	84	87	97±190	56±29	57	10
2010	34±67	16±7.1	99	98	1.2±2.3	2.8±1.9	48	71	130±260	120±33	66	52
2011	15±29	21±16	97	97	1±2.1	1.5±1.7	39	21	83±170	75±27	50	27
2012	11±22	53±13	96	99	0.92±1.8	2±1.6	26	46	74±150	46±27	45	43
2013	16±33	94±13	98	100	1.1±2.1	2.1±1.8	29	48	64±130	110±27	38	22
2014	3.8±7.6	11±6.3	85	94	1.3±2.5	6.8±2.4	35	73	59±120	55±27	35	45
2015	8.7±17	20±12	94	97	1.4±2.7	2.5±2.1	34	37	48±96	19±18	26	9
2016	8.7±17	45±11	94	99	1.4±2.7	3.8±2.2	34	42	48±96	69±24	26	33

790

791

792

793

794

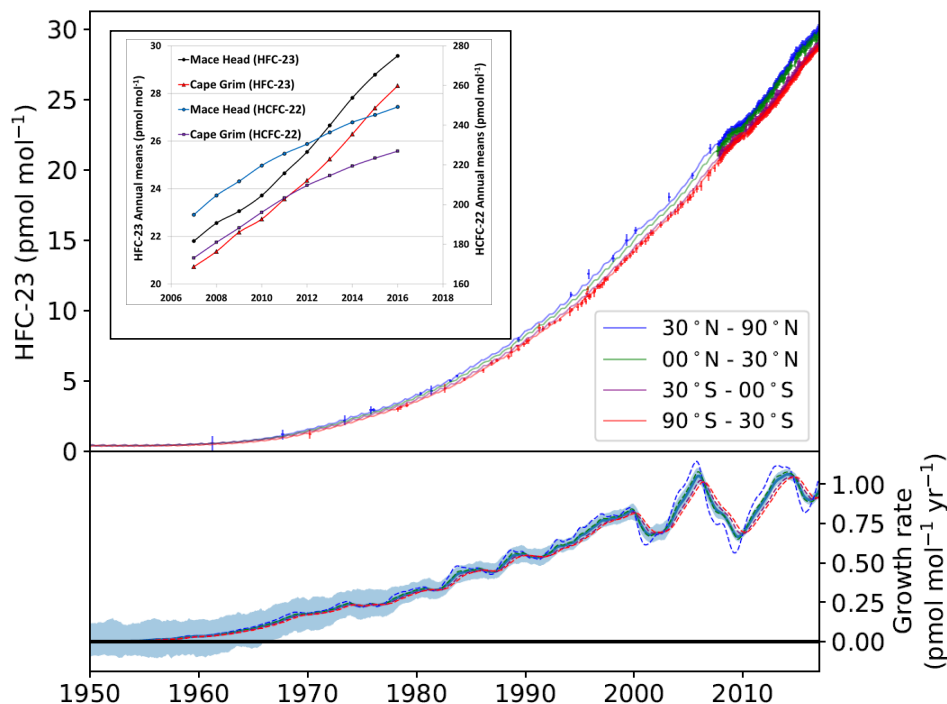
795

796

797

798

799



800

801

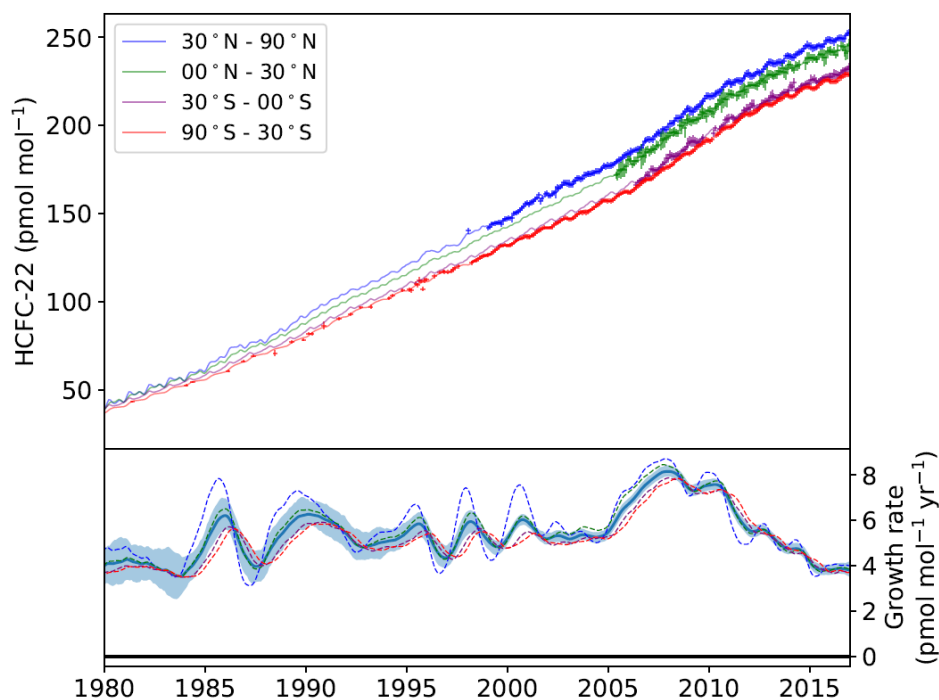
802 Figure 1. HFC-23 modelled mole fractions output for the four equal-mass latitudinal
 803 subdivisions of the global atmosphere calculated from the 12-box model and the in-situ records
 804 from the AGAGE core sites, firn air and CGAA data. Lower box shows the annual growth rates
 805 in $\text{pmol mol}^{-1} \text{yr}^{-1}$. Note: Data are plotted as annual mean mid-year values. Figure 1 inset,
 806 compares the annual mean mole fractions of HFC-23 and HCFC-22 recorded at Mace Head and
 807 Cape Grim from 2007-2016.

808

809

810

811



812

813 Figure 2. HCFC-22 modelled mole fractions for the four equal-mass latitudinal
814 subdivisions of the global atmosphere calculated from the 12-box model and the in-situ records
815 from the AGAGE core sites and CGAA data. Lower box shows the annual growth rates in pmol
816 $\text{mol}^{-1} \text{ yr}^{-1}$. Note: Data are plotted as annual mean mid-year values.

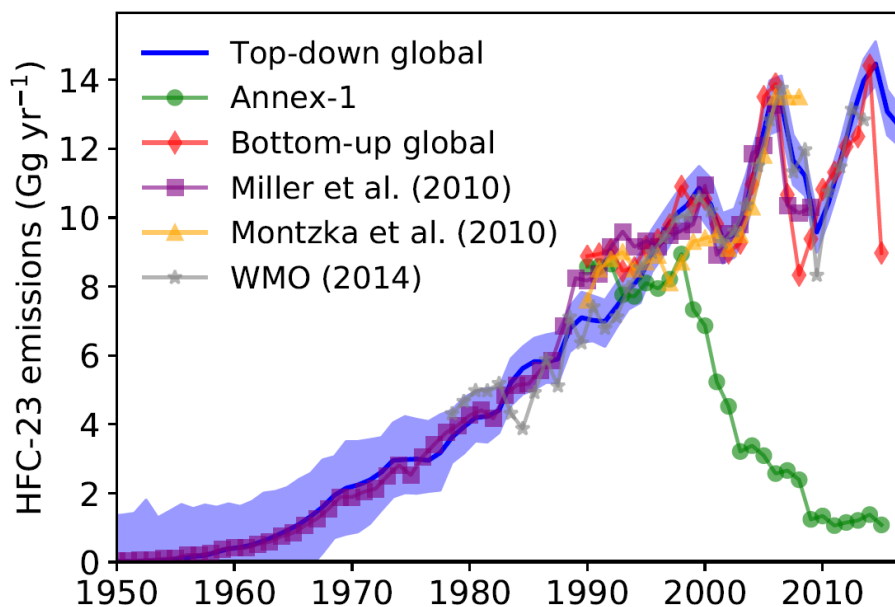
817

818

819

820

821



822

823 Figure 3. Global emissions of HFC-23 calculated from the AGAGE 12-box model (blue line and
824 shading, 1σ uncertainty). Data are plotted as annual mean mid-year values. Data are plotted as
825 annual mean mid-year values. The purple line shows HFC-23 estimates of emissions from Miller
826 et al. (2010), the yellow line HFC-23 emissions estimates from Montzka et al. (2010) and the
827 grey line from Carpenter and Reimann (WMO 2014). The green line shows emissions reports by
828 Annex-1 countries. Red line shows bottom-up estimated global emissions.

829

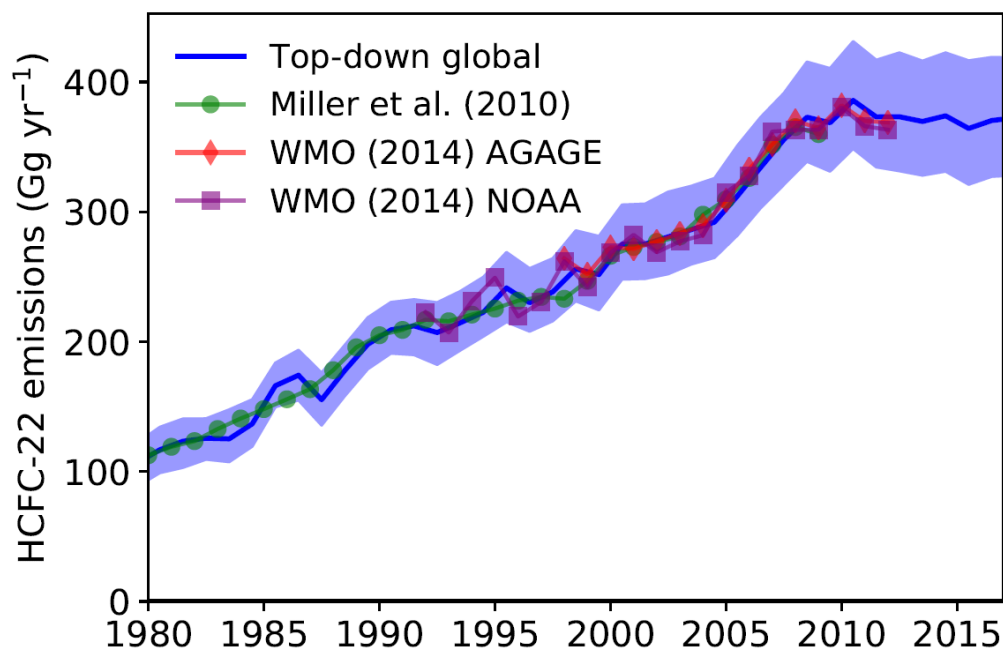
830

831

832



833



834

835 Figure 4. Global emissions of HCFC-22 calculated from the AGAGE 12-box model (blue line
836 and shading, 1σ uncertainty). Data are plotted as annual mean mid-year values. The green line
837 shows bottom-up HCFC-22 estimates of emissions from Miller et al. (2010), Red and purple
838 lines show HCFC-22 emissions for AGAGE and NOAA respectively, reported in Carpenter and
839 Reimann (WMO 2014).

840

841

842

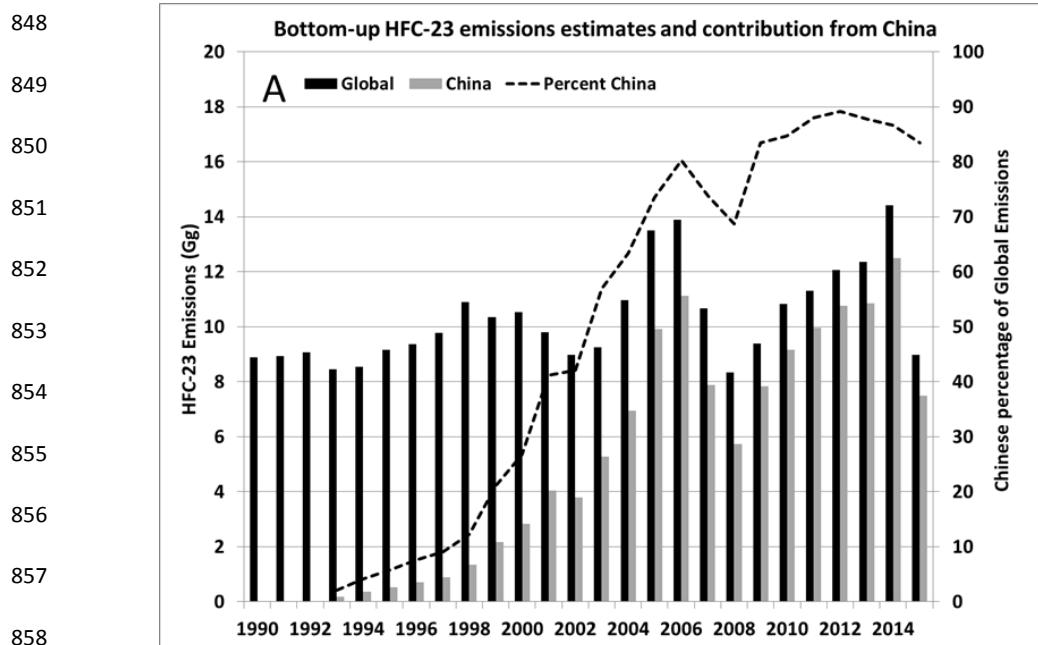
843

844

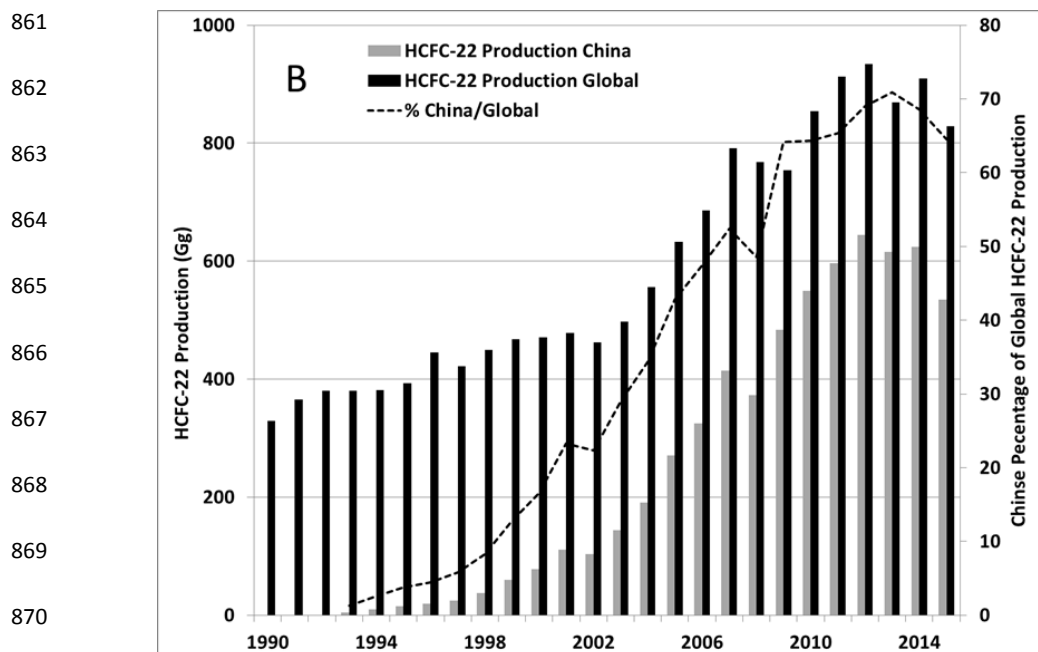
845

846

847



859 Figure 5a. HFC-23 global and Chinese emissions and the percentage of Chinese
860 emissions contributing to the global total (dashed line).



871 Figure 5b. HCFC-22 emissions estimates of global and Chinese production and the
872 percentage of Chinese production as a fraction of the global total (dashed line).

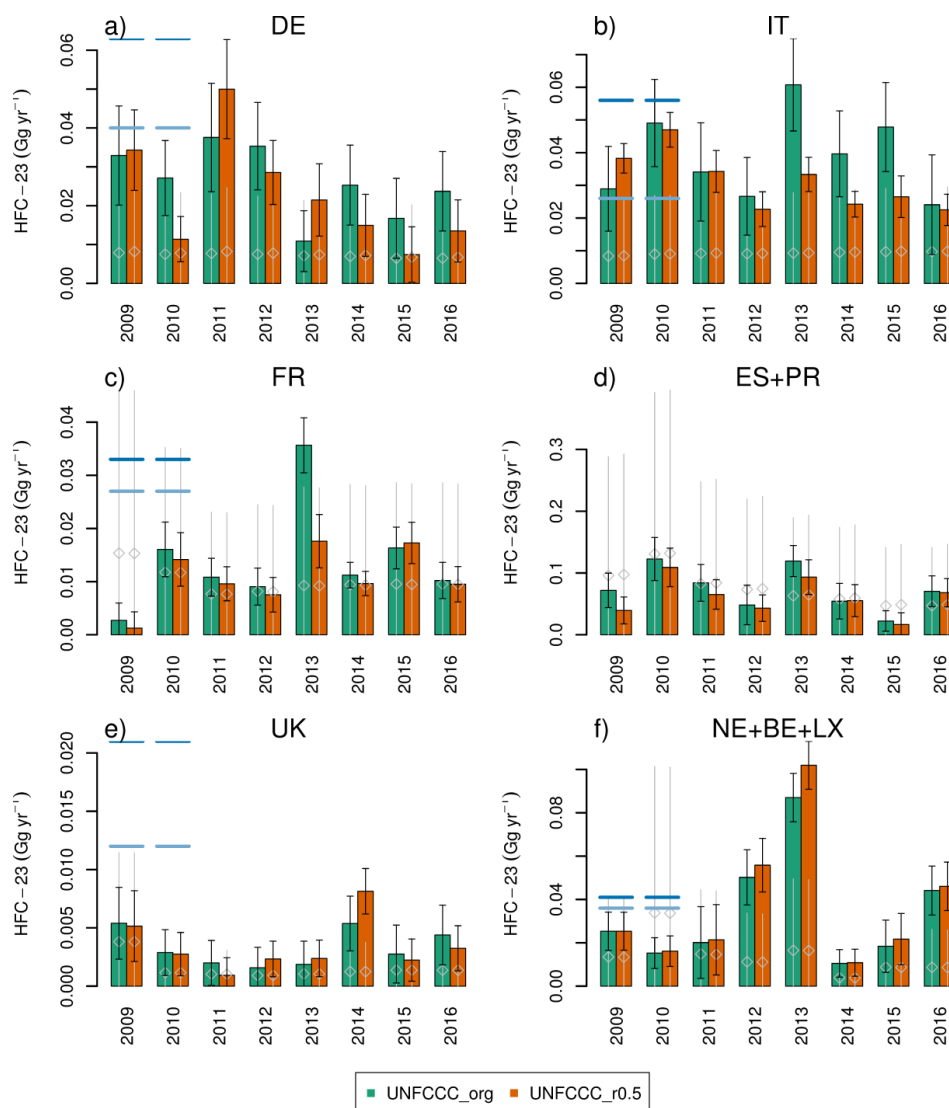


Figure 6: Temporal evolution of national/regional emissions of HFC-23: solid bars and error bars give *a posteriori* emissions using the two sets of *a priori* emissions (grey lines). Blue horizontal lines give the estimates of Keller et al. (2011) for their Bayesian (light blue) and point source (dark blue) estimate; a) Germany (DE), b) Italy (IT), c) France (FR), d) Spain and Portugal (ES+PR), e) United Kingdom (UK), f) Benelux countries (Netherlands, Belgium, Luxembourg, NE+BE+LX).